CTGF/VEGFA-activated Fibroblasts Promote Tumor Migration Through Micro-environmental Modulation*[S]

Wei Wu‡§, Esther A. Zaal‡, Celia R. Berkers‡, Simone Lemeer‡§, and Albert J. R. Heck‡§¶

Fibroblast activation is associated with tumor progression and implicated in metastasis, but the initial triggering signals required to kick-start this process remain largely unknown. Because small cancerous lesions share limited physical contact with neighboring fibroblasts, we reasoned the first tumor-derived signal for fibroblast activation should be secreted and diffusible. By pulsed metabolic labeling and click-chemistry based affinity enrichment, we sieved through the ductal carcinoma secretome for potential fibroblast activators. Using immuno-depletion/supplementation assays on various secreted factors, we pinpointed that tumor-secreted CTGF/VEGFA alone is sufficient to activate paired mammary fibroblasts from the same patient via ROCK1 and JunB signaling. Fibroblasts activated in this manner are distinct in morphology, growth, and adopt a highly tumor-like secretion profile, which in turn promotes tumor migration by counteracting oxidative and lactate stress. These findings reveal a profound division-of-labor between normal and cancer cells under the directive of the latter, and allude to potential metastatic prevention through inhibiting local fibroblast activation. ***Molecular & Cellular Proteomics 17: 1502–1514, 2018. DOI: 10.1074/mcp.RA118.000708.***

Cancer is a disease of immortal cells in the comfort of their tissue microenvironment. The tumor "neighborhood" includes not only endothelial cells and infiltrating immune cells, but also many fibroblasts with poorly characterized functions in tumor progression. The complex multi-way interactions between these cell types ultimately determine tumor proliferation, dissemination and drug response (1, 2). Moreover, the tumor microenvironment is further modulated by secretomes and exosomes of all the cell types present (2, 3), in addition to contact-dependent signaling with the extracellular matrix (ECM) (4). Hence, cancer is hardly a disease of only tumor cells, and there is a growing consensus that cancer therapy should also involve treating the immune system (5–7) and the tumor microenvironment (8).

Favorable conditions in the tumor milieu are even more critical in the context of metastasis, as the existing microenvironment determines largely whether cancer cells could traverse the extracellular matrix (ECM)[1] and gain access to the blood circulation (9). Indeed, tumors that are more tightly encapsulated by ECM are associated with better prognostic outcome (10), whereas the inhibitory role of micro-environmental oxidative stress on tumor migration has been described recently (11). In view of these findings, targeting fibroblasts in the tumor environment should be of therapeutic interest to limit metastatic spread, because these cells that deposit ECM during normal wound healing are also activated in cancer and amplified in number with disease progression (Fig. 1). In line with this, recent publications have noted the supportive role of cancer associated fibroblasts (CAFs) during tumor development (1, 10, 12), but the initial molecular triggers and signaling pathways in activated fibroblasts have remained so far poorly described and largely uninvestigated. Vice versa, the molecular mechanism(s) through which activated fibroblasts promote tumor processes are also essentially unknown.

In consideration of existing models that describe tumor progression, we hypothesized that fibroblast activation could follow two distinct routes. The first involves diffusible molecules of tumor origin that induce activation in a contactless manner; the second requires physical binding between tumor cells and fibroblasts to trigger intracellular signaling events. Because tumors begin as small lesions that contact only a few neighboring fibroblasts, physical interactions between the tumor and fibroblast cells can most likely not account for fibroblast activation and recruitment to tumor site at disease onset. Therefore, we focused on identifying soluble factors from the tumor secretome that could induce fibroblast activation at range and set out to investigate the role of intercellular sig-

From the ‡Biomolecular Mass Spectrometry and Proteomics, Bijvoet Center for Biomolecular Research and Utrecht Institute for Pharmaceutical Sciences, Utrecht University, Padualaan 8, 3584 CH Utrecht, the Netherlands; §Netherlands Proteomics Centre, Padualaan 8, 3584 CH Utrecht, the Netherlands

Received February 26, 2018, and in revised form, April 18, 2018
Published, MCP Papers in Press, April 18, 2018, DOI 10.1074/mcp.RA118.000708

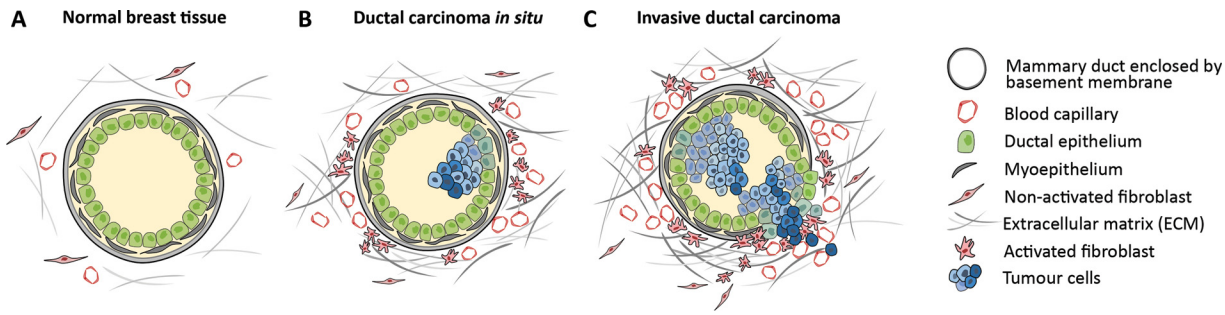

FIG. 1. **Schematic progression of human ductal carcinoma.** *A*, Normal breast tissue. *B*, Ductal carcinoma *in situ*. Fibroblasts are amplified and recruited to tumor site, but remain separated from cancer cells by intact basement membrane. Angiogenesis begins. *C*, Invasive ductal carcinoma. Sustained fibroblast activation and angiogenesis support tumor dissemination. Breach of basement membrane allows physical contact between activated fibroblasts and tumor cells.

naling events between tumor and fibroblast cells, as mediated through secreted molecular entities.

To preserve the required control over experimental conditions, we chose to study tumor-fibroblast interactions in a well-controlled *in vitro* model reconstituted by a pair of tumor and adjacent fibroblast cell lines isolated from the same patient, namely Hs578T and Hs578Bst respectively. This eliminates the complication of forward, reciprocal and sequential signaling that will take place in a living system, to better focus on identifying the first signal(s) that initiate the fibroblast activation process.

We first profiled the ductal carcinoma (Hs578T) secretome, and subsequently used antibody-enabled retrieval/depletion of putative individual fibroblast activators to study their specific effects on the fibroblast activation process. From a panel of secreted factors selected in this manner, we show that tumor-derived connective tissue growth factor (CTGF) and vascular endothelial growth factor (VEGFA) together are already sufficient to induce mammary fibroblast (Hs578Bst) activation. This appears to involve noncanonical *Wnt* mechanisms, where the activities of ROCK and JNK, but not GSK3, are required for morphological transformation and expression of classical activation markers.

More intriguingly, we reveal that fibroblasts activated by CTGF/VEGFA in turn mimic the tumor secretion profile and promote tumor migration by mitigating oxidative stress associated with chemotaxis. These findings describe a profound division-of-labor between normal and cancer cells under the directive of the latter and reaffirm the notion that treating cancer should also involve treating its microenvironment.

MATERIALS AND METHODS

Cell Culture—Paired breast tumor cell line Hs578T and normal breast fibroblast Hs578Bst were obtained from ATCC, tested every 3 months for mycoplasma, and used within passages 5–15 for all experiments. Both cell lines were cultured in Dulbecco's Modified Eagle Medium (DMEM) supplemented with 2 mM L-glutamine, 20 mM HEPES and 10% fetal bovine serum (FBS) in a humidified incubator at 37 °C and 5% CO_2. Cell viability was measured by DNA staining with crystal violet and quantified by absorbance of solubilized crystal violet at 595 nm, and independently verified by classical cell count using a hemocytometer. For AHA labeling, fresh Azido-homoalanine was supplemented to 0.1 mM final concentration.

Fibroblast Activation—Hs578T cells were seeded at 25% confluency and allowed to adhere for 24 h before growth medium was replaced. Hs578T cells were then allowed to secrete for 24 h before the conditioned medium was pelleted at 4000 × *g* for 10 min, and the supernatant added to Hs578Bst cells seeded 48 h before. After incubating Hs578Bst cells in Hs578T conditioned media for 48 h, fibroblast activation was verified in every experiment visually by microscopic morphology and experimentally by probing for activation markers SMA and S100A4. To test for reversal of activation, activated fibroblasts were re-plated in fresh medium for 2, 4, 6, or 14 days without activating stimulus from Hs578T cells. All subsequent experiments were performed within 4 days post-activation.

Cell Migration and Invasion—Migration inserts with 8 μM pores (Falcon, NJ) were coated on the underside with 10 ng/μl Fibronectin (Sigma-Aldrich, MI) overnight at 4 °C. In each migration insert, 2×10^4 Hs578T cells were seeded and allowed to migrate for 3 h toward an FBS chemoattractant gradient in the lower chamber that contained either fresh medium, 1×10^4 Hs578Bst cells in fresh medium, 1×10^4 activated Hs578Bst+ cells in fresh medium, or conditioned medium from 1×10^4 activated Hs578Bst+ cells. Matrigel invasion inserts with 8 μM pores (BD, NJ) were rehydrated in serum-free medium for 2 h at 37 °C, and washed twice with serum free medium. In each invasion insert, 1×10^5 Hs578T cells were seeded and allowed to invade across matrigel for 20 h toward the same conditions in the lower chamber. Cells that remained in the inserts were removed by PBS cotton swab, whereas cells that have migrated or invaded to the bottom side of the insert were fixed with 4% paraformaldehyde, stained with 0.5% crystal violet in 20% methanol, visualized by microscopy, and subsequently quantified by crystal violet solubilization in 1% SDS and spectrophotometric reading at 595 nm. Normalization by taking fold change was performed with respect to migrating Hs578T cells in fresh medium, in the absence of TBHP, GSH or conditioned medium (dash line reference in Fig. 2*E*–2*F*; Fig. 7*C*).

Western Blotting—Cells were lysed by gentle vortexing cycles of 3 × 10s in 8 M urea, 50 mM ammonium bicarbonate and 0.5% sodium deoxycholate supplemented with 50 μg/ml each of DNase I and RNase A (Sigma-Aldrich), and inhibitor cocktails against proteases and phosphatases (Roche, Basel, Switzerland). Insoluble cell debris was pelleted at 20,000 × *g* for 60min and protein content of soluble

[1] The abbreviations used are: ECM, extracellular matrix; AHA, Azido-homoalanine; CM, conditioned medium; CTGF, connective tissue growth factor; IP, immunoprecipitation; ROS, reactive oxygen species; SMA, smooth muscle actin; VEGFA, vascular endothelial growth factor A; WCL, whole cell lysate.

fraction was estimated by Bradford protein assay (Bio-Rad, CA). On total cell lysates of 20 μg protein load, all primary antibodies (Santa Cruz, CA) were used at 1:500 dilutions for overnight incubations at 4 °C. Antibodies against SMA, S100A4, LTBP1 and IL8 were raised in mouse; antibodies against ANGP1, VEGF and tubulin in rabbit; and antibodies against CTGF and SCG2 in goat. The respective secondary antibodies conjugated with HRP (Dako, Santa Clara, CA) were used at 1:2000 dilution. On 10 μl conditioned medium, primary antibodies were used at 1:50 and secondary antibodies at 1:500. Western signals were visualized using SuperSignal West Dura extended duration chemiluminescent substrate (Thermo Scientific, MA) on a GeneGnome imager (Syngene, Cambridge, UK).

Immunoprecipitation—For immuno-depletion from Hs578T conditioned medium, 60 μg of each antibody was crosslinked to 5 μl Protein A/G agarose beads (Santa Cruz) with 450 μM disuccinimidyl suberate (Thermo Scientific). Uncrosslinked antibodies were removed with 0.1 M glycine, pH 3, and the beads were equilibrated twice in full DMEM medium for 5 min. Depletion of secreted proteins LTBP1, IL8, ANGP1, VEGFA, CTGF, or SCG2 from Hs578T conditioned medium was performed three times sequentially, each for 30 min with end-to-end rotation at room temperature. Immunoprecipitated proteins were recovered by glycine elution and neutralized immediately with sterile 1 M Tris-HCl, pH 9. Because antibodies against LTBP1 and IL8; ANGP1 and VEGFA; and CTGF and SCG2 were raised in the same host animal and isotype-matched, they acted as control immunoprecipitations for each other. In supplementation experiments, the immunoprecipitated proteins from Hs578T conditioned medium were neutralized and added directly to Hs578Bst conditioned medium. For CTGF/VEGFA and SCG2/ANGP1 double depletion and supplementation, antibody-coated beads were mixed after preparation and added to Hs578T conditioned medium together in a single step.

CTGF Antibody Blocking—Hs578Bst cells were seeded in 24-well format in fresh medium. After 48 h, medium was removed and adherent cells were washed on-the-plate with PBS containing 0.1 μg/ml antibody against CTGF or SCG2 as IgG control. Subsequently, 0.5 ml Hs578Bst conditioned medium or Hs578T conditioned medium supplemented with 6 μg antibody against CTGF or SCG2 were added. After a further 48 h, Hs578Bst cells were imaged and harvested for western detection of SMA and S100A4 to test for fibroblast activation.

AHA Labeling, Enrichment, and Digestion of Secreted Proteins—Cells were seeded at 20% confluency and allowed 48 h to adhere in full growth medium (DMEM+10%FBS). Cells were starved in DMEM+10% FBS-methionine for 1 h, after which methionine analogue azido-homoalanine (AHA) (Bachem, Bubendorf, Switzerland) was re-introduced to a final concentration of 0.1 mM. In DMEM+10% FBS+AHA, cells were allowed 24 h to synthesize and secrete new proteins that have incorporated azide functional groups into the culture medium. In each biological replicate, 15 ml of conditioned medium was concentrated to 250 μl by 3 kDa molecular weight cutoff filters (MerckMillipore, Darmstadt, Germany) and azide-labeled proteins were covalently linked to alkyne beads via click chemistry as described previously (13), with modifications. Proteins on beads were extensively washed with ionic (250 mM NaCl, 1% SDS) and denaturing (8 M Urea, 50 mM ammonium bicarbonate) buffers to eliminate secondary interactions between secreted proteins and FBS proteins. Proteins were then reduced in 10 mM DTT at 70 °C for 15min, alkylated in 20 mM iodo-acetamide (IAA) at 20 °C for 30min in the dark, and digested from beads with 0.5 μg trypsin (Sigma-Aldrich) for 12 h at 37 °C. Digested peptides were purified by c18 ZipTips (MerckMillipore) before LC-MS/MS analyses and database search.

LC-MS/MS Protein Identification and Quantification—Secretome samples were analyzed using an UHPLC 1290 system (Agilent, Santa Clara, CA) coupled to an Orbitrap Q Exactive Plus mass spectrometer (Thermo Scientific), in data-dependent acquisition mode, largely as described previously (14). Briefly, peptides were first trapped on a 2 cm × 100 μm Reprosil C18 precolumn (3 μm) and then separated on a 50 cm × 75 μm Poroshell EC-C18 analytical column (2.7 μm) over a 120 min gradient. Trapping was performed for 10 min in 0.1 M acetic acid (Solvent A) and elution with 80% ACN in 0.1 M acetic acid (Solvent B) in gradients as follows: 13–40% solvent B in 95 min, 40–100% in 3min, hold at 100% for 1min and finally equilibration back to 0% solvent B for 11 min. Flow was passively split to 350 nl/min. MS data were obtained in data-dependent acquisition mode. Full scans were acquired in the m/z range of 375–1600 at the resolution of 35,000 (*m/z* 400) with AGC target 3E6 in the maximum filling time of 250ms. Top 15 most intense multiply charged precursor ions in the *m/z* range of 200–2000 were selected for HCD fragmentation performed at resolution of 17,500 using NCE 25%, after accumulation to target value of 5E4 in the maximum filling time of 120 ms. Dynamic exclusion was set to 18 s.

Raw files were processed using MaxQuant version 1.5.3.30 and the Andromeda search engine, against the human (147933 entries) Uniprot database (version Jan 2016) concatenated to bovine-specific portion (32166 entries) of the database. Enzyme specificity was set to Trypsin, and up to 2 missed cleavages were allowed. Cysteine carbamidomethylation was set to fixed modification, whereas variable modifications of methionine oxidation and protein N-terminal acetylation were allowed, together with either methionine to AHA substitution (secretomics), or phosphorylation of Ser, Thr, Tyr (STY) residues (phosphoproteomics). False discovery rate (FDR) was restricted to 1% in both protein and peptide identification. Precursor mass deviation was 4.5ppm, whereas fragment mass deviation was allowed up to 20ppm. Because click-chemistry based enrichment of secreted proteins always results in the loss of one peptide that is permanently "clicked" to alkyne beads, protein identification in the secretome experiment was filtered based on one unique peptide, with at least two peptide spectra matches (PSMs). For quantitative secretome comparisons between Hs578Bst, activated Hs578Bst+ and Hs578T tumor cells, label-free quantification (LFQ) was performed with "match between runs" enabled. Secreted protein abundance ratios were calculated by taking the nonactivated Hs578Bst secretome as reference.

Prior to total proteome analyses, each sample was prefractionated by high pH reverse-phase HPLC. Peptides were trapped in 20 mM NH4OH, pH10 (Solvent A), eluted in 80% ACN, 20 mM NH4OH, pH10 (Solvent B), and concatenated into 5 fractions for second dimensional LC separation over a 120 min gradient, and MS analyses as described above. Prior to phosphoproteome analyses, phosphopeptides in whole cell digests were enriched by Ti^{4+}-IMAC as described previously (15).

Inhibitor Treatments—Small molecule inhibitors against GSK3 (GSK3*i*; CHIR-98014), JNK (JNK*i*; SP600125), and ROCK (ROCK*i*; GSK269962) were purchased from SelleckChem (Houston, TX). GSK3*i*, JNK*i* and ROCK*i* were used at 1 μM, 2 μM and 5 μM respectively in actual inhibition experiments, and half the dose was used in pretreatments. Nonactivated fibroblasts were allowed 48 h to attach at 15% confluency in 48-well plates and pretreated with respective inhibitors for 24 h. Fresh inhibitors were added when culture medium was replaced with Hs578T conditioned medium or supplemented with CTGF/VEGFA immuno-precipitated from Hs578T conditioned medium. Fibroblasts were next monitored by phase-contrast microscopy and lysed for western detection of activation markers after 48 h. Fibroblast cell viability exceeded 95% after 24-hour pretreatment and 48-hour activation, compared with DMSO control.

Experimental Design, Statistical Rationale and Data Visualization—Phase-contrast images were taken using a Nikon Eclipse TS100 light microscope with 10x magnification, at equal and low density of 20–30% to preserve cell morphology. Representative raw images from

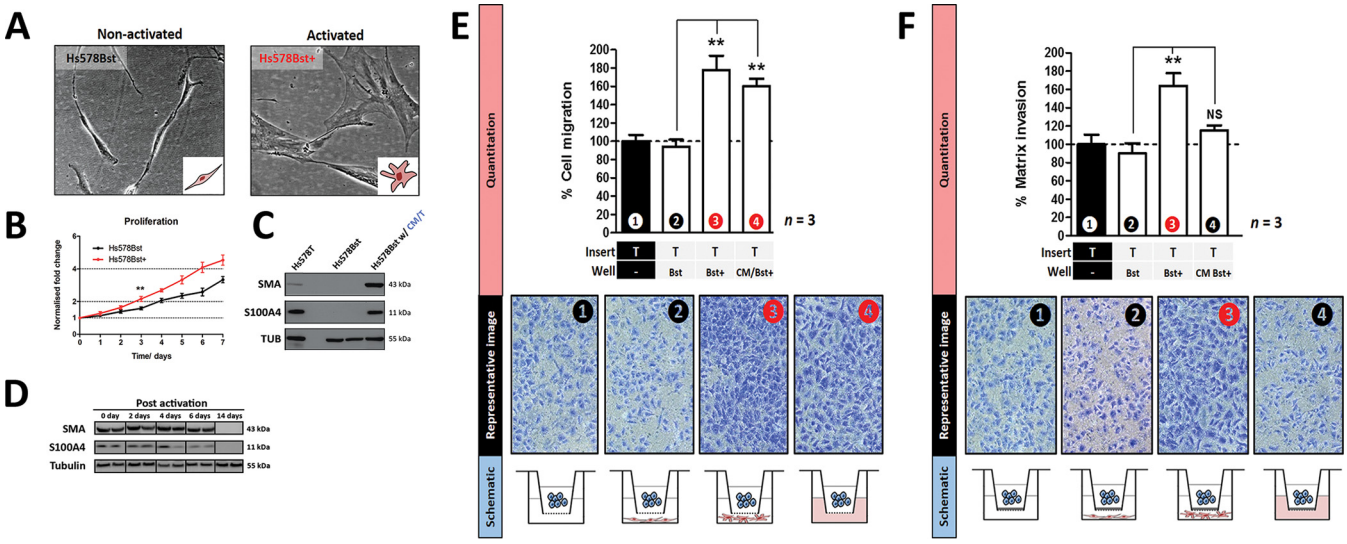

FIG. 2. **Fibroblast activation by tumor secretions.** *A*, Morphology. Nonactivated fibroblasts (Hs578Bst, left) are long and tubular whereas activated fibroblasts (Hs578Bst+, right) are larger with more stress fibers and morphologically distinct. Inset: pictorial representation of Hs578Bst and Hs578Bst+ cells. *B*, Proliferation. Hs578Bst+ cells grow significantly faster than nonactivated Hs578Bst cells from 72 h onwards (Student's *t* test; $^{**}p < 0.01$; $n = 7$). *C*, Activation markers. Expression of smooth muscle actin (SMA) and S100A4 were observed after 72-hour incubation in Hs578T tumor conditioned medium. *D*, Reversal of fibroblast activation. Upon removal of Hs578T tumor conditioned medium, Hs578Bst+ cells gradually lost the expression of activation markers over 6–14 days. *E*, Transwell migration. When co-cultured with Hs578Bst+ cells or Hs578Bst+ secretions, Hs578T cells migrated significantly more in 3 h compared with when cocultured with Hs578Bst cells (Student's *t* test; $^{**}p < 0.01$; $n = 3$). *F*, Matrix invasion. When cocultured with Hs578Bst+ cells, Hs578T cells invaded significantly more in 20 h compared with when cocultured with nonactivated Hs578Bst cells (Student's *t* test; $^{**}p < 0.01$; $n = 3$).

quadruplicates were used in figures, without contrast adjustments. To account for biological variation, all experiments involving induction of fibroblast activation, cell migration and invasion, antibody blocking, GSH and TBHP treatment, and chemical inhibition of *Wnt* signaling were performed in at least 3 biological replicates starting from different stocks of Hs578Bst and on different days. Statistical significance within each experimental replicate was assessed by Student's *t* test (two-tailed, paired). Error bars indicate experimental standard deviation.

All mass spectrometry experiments were performed in biological triplicates starting from separate cultures, considering intrinsic biological variation should supersede technical variation in the approaches taken for analysis. Pearson correlation of all biological replicates (secretome, proteome and phosphoproteome) within the same experimental category exceed 0.9, and no sample was omitted in analysis. In discovery of secreted proteins from Hs578T cells, stringent cutoff for identification in all three biological replicates was used without imputation, as only targets that were consistently detectable could be studied further in relation to fibroblast activation. In secretome comparisons, imputation was only performed on a maximum of one out of three biological replicates within each comparison group. This imposes control over imputed data but still allows robust statistical filtering from a large dataset based on fold change and *t* test statistics.

Secreted proteins were annotated based on UniProt sequence features and SwissProt Protein Information Resource (PIR) keywords. Presence of signal peptides were verified with SignalP 4.1, and non-cannonical secretion was cross-validated against ExoCarta. Gene ontology analysis based on cellular compartment was performed with Gene Ontology enRIchment anaLysis and visuaLisAtion (GORILLA) tool, whereas biological processes were visualized by Database for Annotation, Visualization and Integrated Discovery (DAVID, version 6.7). Changes in intracellular metabolites and metabolic uptake from culture medium were visualized with MeV software version 4.8.1. All data bar charts were plotted using Graphpad PRISM 7.

RESULTS

Nomenclature—For clarity, we define first the nomenclature used to refer to cell types studied: *Hs578T*; breast cancer cell line derived from a female Caucasian patient. *Hs578Bst*; fibroblast cell line isolated from the tumor periphery of the same patient. *Hs578Bst+*; *Hs578Bst* fibroblasts activated by secreted factors from *Hs578T* cells.

Contact-independent Fibroblast Activation by Tumor-secreted Factors—To test if Hs578T breast cancer cells could indeed activate paired fibroblasts (Hs578Bst) via secreted factors, we cultured these fibroblasts in Hs578T conditioned medium for up to 5 days and assayed for changes that indicate activation. As shown in Fig. 2, after a two-day incubation in the tumor secretome, Hs578Bst fibroblasts showed about 30% increase in growth (Fig. 2*A* and 2*B*), profoundly different morphology with increased cell size, more evident stress fibers and cell spreading (Fig. 2*A*), as well as the expression of classical activation markers smooth muscle actin (SMA) and S100A4 (Fig. 2*C*). Together these observations demonstrate that secreted factors of tumor origin could initiate fibroblast activation in a contact-independent manner, and that initiating factors for this process are contained in the tumor secretome.

More importantly, these activated fibroblasts (Hs578Bst+) significantly promoted tumor migration (Fig. 2*E*) and invasion (Fig. 2*F*) in contactless co-cultures, suggesting that fibro-

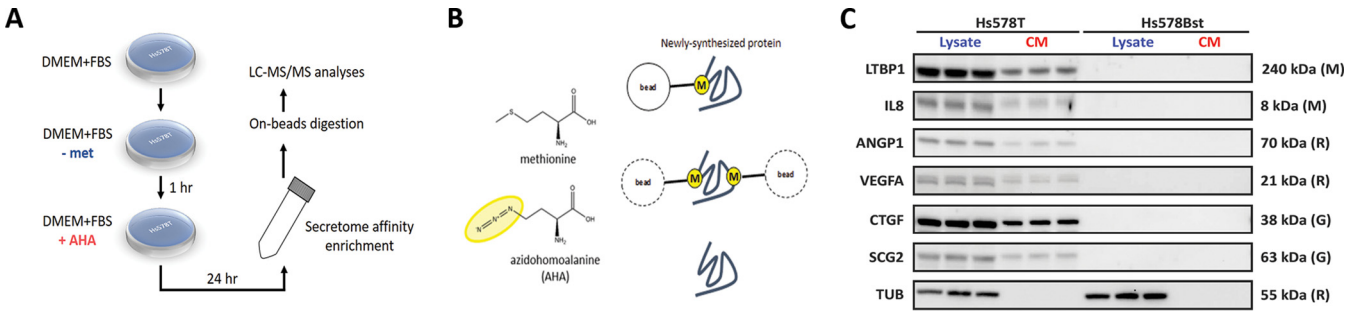

FIG. 3. **Identification of potential tumor-derived fibroblast activators.** *A*, Workflow schematic. Methionine starvation was performed for 1 h to use up >90% of intracellular methionine (supplemental Fig. S5). *B*, Structures of methionine and AHA. Newly synthesized and secreted proteins containing at least 1 AHA substitution may be covalently linked to alkyne beads; secreted proteins devoid of methionine residues are not enriched by this method. *C*, Differential expression and secretion. Six potential targets were specifically expressed and secreted by Hs578T cells but not Hs578Bst cells. CM; conditioned medium. M, R, G in parentheses; antibodies raised in mouse, rabbit and goat respectively. Full list of proteins secreted by Hs578T cells in supplemental Table S1.

blasts activated by tumor-derived factors have pro-metastatic function and in turn support dissemination of the tumor cells in a positive feedback manner. In addition, we also show that fibroblasts activated in this manner could revert to the non-activated state in 4 to 6 days upon removal of activating stimulus, *i.e.* the Hs578T conditioned medium (Fig. 2*D*). This implies that therapeutic reversal of fibroblast activation may be possible through neutralizing the tumor-derived stimulus, which may be clinically relevant in cancer therapy.

Identification of Potential Fibroblast Activators—To pinpoint proteinaceous component(s) in the tumor secretome that could be responsible for fibroblast activation, we screened through the Hs578T secretome, using pulsed metabolic labeling, azide-alkyne click chemistry-based affinity capture and finally mass spectrometry (13) (Fig. 3*A* and 3*B*). This approach simultaneously overcomes the limitations of low analyte concentration and FBS contamination in standard secretome workflows. By stringent filtering for identification in 3 out of 3 biological replicates and at least 1 AHA-containing peptide to exclude FBS contaminants, we obtained a smaller but highly confident list of 324 secreted proteins from Hs578T cells (supplemental Table S1). Among these, 95% were annotated with the GO terms "secreted" (294), "extracellular" (6) or documented in the ExoCarta database (7), and 68% of these contain classical signal peptides (supplemental Fig. S1*A*), suggesting these proteins are targeted for extracellular function. In addition, >50% of all identifications feature sequence motifs that indicate *N*-linked glycosylation and disulfide bonds, which are structural modifications highly prevalent in secreted proteins (supplemental Fig. S1*B*). Gene ontology analyses of proteins identified in the Hs578T secretome were also consistent with extracellular function (supplemental Figs. S1*C* and S1*D*). Together, these provide excellent support for specific enrichment and identification of proteins from the Hs578T secretome, which contains potential fibroblast activators.

To trim the data set toward a manageable number of putative fibroblast activators for individual functional testing, we employed a series of filtering criteria to retain potential targets that are: (1) chemoattractant; (2) mitogenic; (3) morphogenic; (4) angiogenic; or (5) involved in TGFβ signaling, which has been implicated in fibroblast activation previously (16). We devised these criteria in view of the patho-histological evidence accumulated in cases of breast cancer (17), where activated fibroblasts are (1) recruited from distant sites; (2) induced to proliferate; (3) morphologically distinct; and (4) observed concurrently with vessel formation prior to metastasis. In addition to these, we also paid attention to soluble cytokines that function largely without known cofactors. With these criteria, we shortlisted 17 putative fibroblast activators (in gray; supplemental Table S1). Dependent on antibody availability, the specific expression and secretion of 6 of these proteins by Hs578T tumor cells were validated (Fig. 3*C*).

CTGF and VEGFA Induce Fibroblast Activation—To confirm fibroblast-activating properties, we designed an immunoprecipitation (IP) strategy, to assess both induction and inhibition of fibroblast activation, with factor supplementation or depletion, respectively (Fig. 4*A*). Systematically, we depleted the Hs578T conditioned medium of each of the 6 putative fibroblast activators and added the flow-through to Hs578Bst fibroblasts to test for loss of activation. In parallel, we eluted the antibody-bound putative factors and added each of these to Hs578Bst fibroblasts to test for activation. Immuno-depletion was successful in 5 out of 6 chosen protein targets, namely LTBP1 and IL8 using mouse antibodies; ANGP1 and VEGFA using rabbit antibodies; and CTGF using goat antibody (Fig. 4*B*). The SCG2 pull-down was unsuccessful but still included as a goat IgG control for CTGF depletion. Success and specificity of immuno-precipitations was also confirmed independently by MS analyses of the IP eluates.

Using this strategy, we observed that depletion of either VEGFA or CTGF blocked fibroblast activation that is normally induced by Hs578T conditioned medium in 2 days (Fig. 5A, panels ⓬ to ⓯), although some morphological changes after day 5 were still noted when CTGF was depleted with VEGFA still present (Fig. 5*A*, panel ⓯). Notably, supplementing

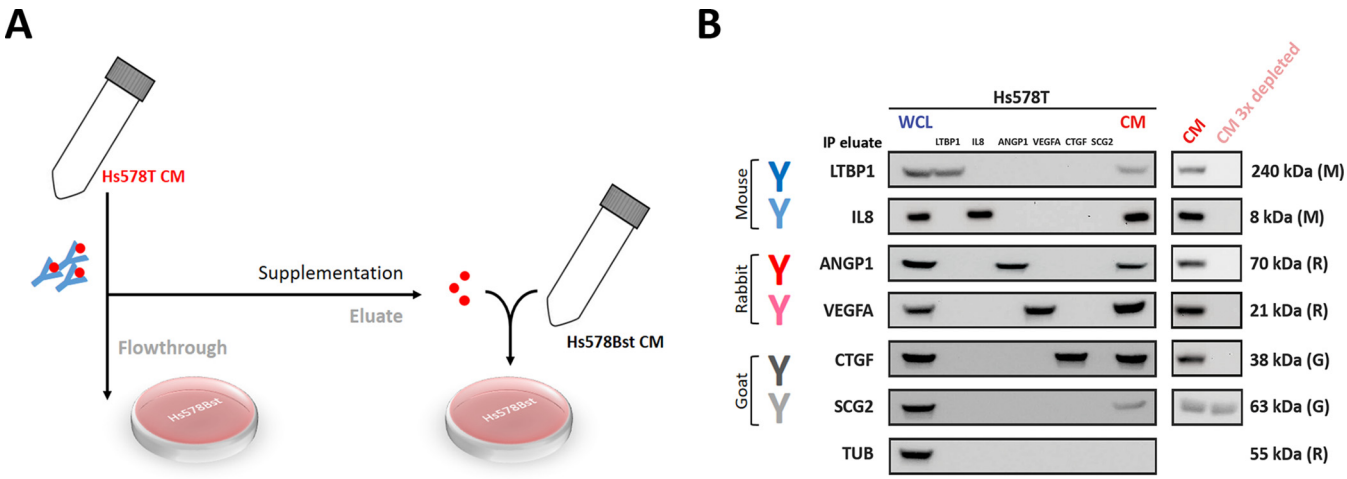

FIG. 4. **Fibroblast activator depletion/supplementation strategy.** *A*, Workflow schematic. Conditioned medium from Hs578T tumor cells was harvested after 24 h and separately depleted of each putative fibroblast activator by immunoprecipitation. Each depleted flowthrough was added to Hs578Bst cells to assay for loss of fibroblast activation. Target proteins eluted from beads were added to Hs578Bst cultures to assay for induction of activation. *B*, Western confirmation of immuno-depletion. Whole cell lysate (WCL) and conditioned medium (CM) were included as controls. LTBP1, IL8, ANGP1, VEGFA and CTGF were successfully depleted from Hs578T conditioned medium (right panel), and detected in IP eluates (left panel).

VEGFA alone induced morphological changes only in 5 days without expression of activation markers, whereas addition of CTGF alone produced no morphological change but weak expression of SMA (Fig. 5*B*, panel ❺ and ⓯). Collectively these suggest that fibroblast activation might require a two-component system, where CTGF initiates the activation process, and VEGFA is required for full morphological transformation. Addition of LTBP1, IL8, or ANGP1 (Fig. 5*A*), or depletion of these factors from full tumor conditioned medium (Fig. 5*B*) had no observable effects on fibroblast activation, in terms of morphology, growth, and expression of activation markers, suggesting that these factors are not involved in the core activation process.

Because both CTGF and VEGFA appear to be needed for full fibroblast activation, we adapted the same strategy for double depletion/supplementation of CTGF and VEGFA, where antibodies against each factor were cross-linked to agarose beads in bulk, and premixed before a single depletion experiment. Using this approach, we observed that fibroblast activation is fully reconstituted in 2 days by the addition of CTGF/VEGFA retrieved simultaneously from the tumor conditioned medium (Fig. 5*C*), suggesting the activation process was largely dependent on CTGF and VEGFA secreted from Hs578T cells. Notably, fibroblasts activated by the combination of CTGF and VEGFA were indistinguishable from fibroblasts activated by the full tumor conditioned medium based on assessment of morphology, activation markers (Fig. 5*C*), as well as growth and the ability to promote tumor migration and invasion *in vitro* (supplemental Fig. S2*A*–S2*C*). Neutralizing CTGF with antibodies supplemented directly to the tumor conditioned medium was sufficient to block fibroblast activation (Fig. 5*D*), further supporting that CTGF is the dominant factor required to initiate fibroblast activation.

The expression and secretion of CTGF and VEGFA were also validated in 5 other primary breast cancer cell lines, namely BT474, MDA-MB-231, HCC1954, HCC1419, and HCC202, across different breast cancer subtypes (triple-negative or Her2-positive), genetic backgrounds and ethnic origins (supplemental Fig. S3), suggesting in addition that tumor-secreted CTGF/VEGFA might be a conserved fibroblast activation signal in breast cancer. This is further supported by immmuno-histochemical evidence from The Human Protein (Cancer) Atlas (18); breast tumors stain positive for CTGF and VEGFA in the cancerous core, peri-cellular space and adjacent connective tissues, providing further validation that CTGF and VEGFA are expressed and secreted by breast tumors *in vivo* (Appendices 1 and 2).

CTGF/VEGFA Activate Fibroblasts Via ROCK1 and JunB Signaling—To reveal further the mechanism of fibroblast activation and molecular consequences of this process, we combined multiple "—omics" strategies to comprehensively profile for changes in the fibroblast proteome, phosphoproteome and metabolome upon activation. Using quantitative phospho-proteomics, we detected significant increase in phosphorylation on Rac1, Jnk1, JunB, and ROCK1 in activated Hs578Bst+ fibroblasts (Fig. 6*B*; supplemental Fig. S2*B*). Collectively, these support potential activation of *Wnt* signaling through Rho- and Rac-dependent routes (Fig. 6*C*). These findings are novel yet consistent with existing literature reports of RhoA regulating S100A4 transcription (19). In further support of our proposed model, treatment with ROCK*i* (GSK269962) and JNK*i* (SP600125) strongly inhibited fibroblast activation, with consequently no detectable expression of activation markers (Fig. 6D), or morphological transformation (Fig. 6*E*). The activation mechanism also appears to be independent of β-catenin mediated transcription, because

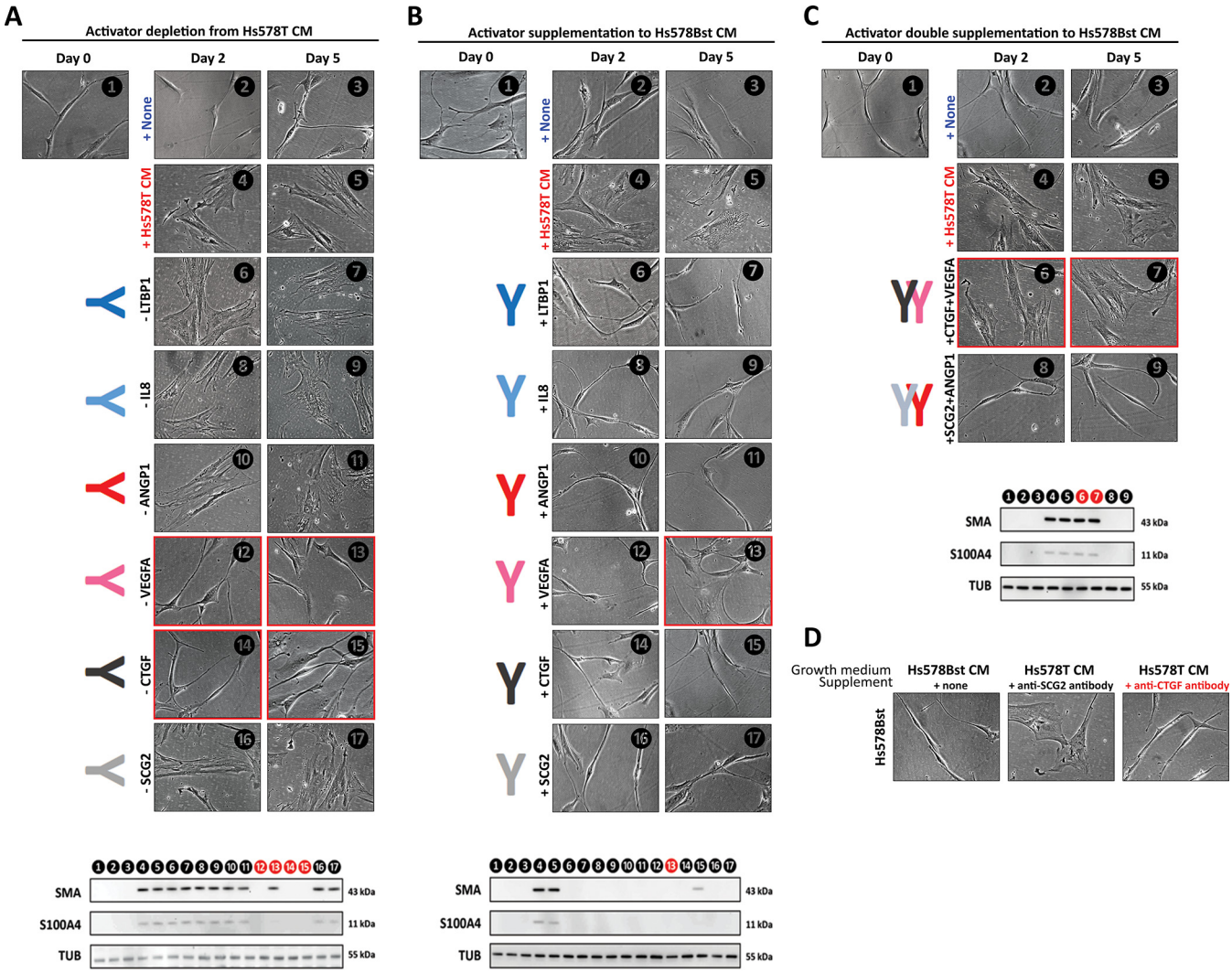

FIG. 5. **Two-component fibroblast activation system.** 1 to 3: negative controls for fibroblast activation; 4 and 5: positive controls for fibroblast activation with full Hs578T conditioned medium in 2 and 5 days respectively. *A*, Activator depletion. Specific removal of CTGF or VEGFA from Hs578T conditioned medium abolished the ability to activate Hs578Bst fibroblasts in 2 days or 5 days 12 to 15). *B*, Activator supplementation. Addition of immuno-precipitated CTGF or VEGFA alone induced very weak activation only after 5 days 13 and 15). *C*, Double supplementation of CTGF and VEGFA. Addition of simultaneously immuno-precipitated CTGF and VEGFA induced full fibroblast activation after 2 days 6 and 7) but not in isotype-matched antibody controls 8 and 9). *D*, Antibody neutralization. Preincubation of CTGF antibody with Hs578T conditioned medium was sufficient to block fibroblast activation.

inhibition of GSK3 activity with CHIR-98014 had no apparent effect on fibroblast activation, or the sustenance of fibroblast activated state (supplemental Fig. S6). Taken together, these data support a novel tumor-dependent fibroblast activation model mediated, at least in part, through the function of Rock1 and JunB, and provide evidence for the existence of paracrine activation mechanisms through secreted CTGF/VEGFA.

Activated Fibroblasts Promote Tumor Migration by Mitigating Oxidative Stress—Although activated fibroblasts consumed significantly more metabolites from the medium and apparently utilized the amino acids assimilated (supplemental Fig. S2*C*), these additional nutrients did not translate into the synthesis of specific proteins that could shed light on pro-metastatic function (supplemental Fig. S4*B*, supplemental Table 1). Widespread phosphorylation changes were observed after 2-day incubation in Hs578T conditioned medium (supplemental Fig. S2*B*), but modulated phospho-signaling alone could not account for increased metabolic uptake. Given these observations, we questioned if the nutrients were used to synthesize proteins that were excreted, and thus "lost" from the whole-cell proteome.

We compared the secretomes of Hs578T tumor cells, and Hs578Bst fibroblasts with or without prior activation by tumor-derived CTGF/VEGFA (Fig. 7). With respect to nonactivated fibroblasts, 57 proteins were differentially secreted after activation (Fig. 7A; in bold, supplemental Table S1). Among these are (1) enzymes and core proteins that modify the cell

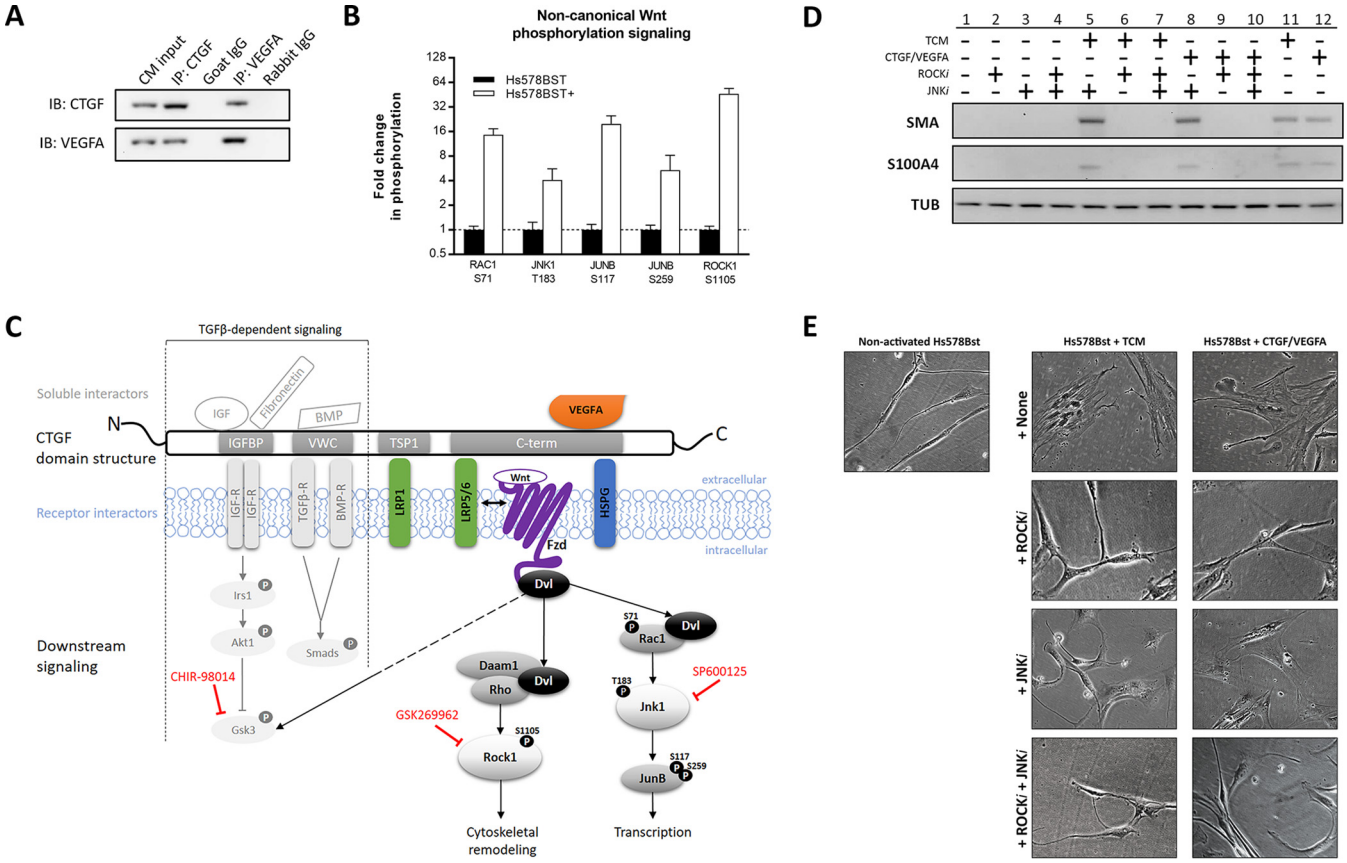

FIG. 6. **CTGF/VEGFA induce fibroblast activation via noncanonical *Wnt* signaling.** *A*, CTGF and VEGFA reciprocal co-immunoprecipitation. CTGF interacts with VEGFA extracellularly in Hs578T conditioned medium (CM) harvested after 3 days. *B*, Fold change in phosphorylation of *Wnt* targets measured by phosphoproteomics. Phosphosite localization probabilities of RAC1 (S71), JNK1 (T183), JUNB (S117, S259) and ROCK1 (S1105) >0.8; fold changes in phosphorylation are statistically significant by paired *t* test ($p < 0.01$; $n = 3$) (supplemental Fig. S2*B*). *C*, Schematic of noncanonical *Wnt* signaling downstream of CTGF/VEGFA-mediated fibroblast activation. No phosphorylation changes were detected in Smad2, Smad3 and Gsk3 by phosphoproteomics, or in Akt1 by Selective Reaction Monitoring (SRM). CHIR-98014, GSK269962 and SP600125 (in red) inhibit the activities of Gsk3, Rock1 and JunB respectively. Gsk3 inhibition had no effect on fibroblast activation, and no effect on the sustenance of activated fibroblast phenotype (supplemental Fig. S6). *D*, ROCK and JNK inhibition. Incubation with Hs578T conditioned medium (TCM) or CTGF/VEGFA activates fibroblasts (lanes 11–12). Treatment with ROCK*i* (5 μM) and JNK*i* (2 μM) has no effect on nonactivated Hs578Bst in the absence of tumor conditioned medium or CTGF/VEGFA (lanes 1–4). Inhibition of ROCK and JNK blocks fibroblast activation by TCM or CTGF/VEGFA (lanes 5–10). *E*, Fibroblast morphology. ROCK and JNK inhibition on fibroblasts abolished morphological changes associated with activation.

surface sulfation and proteoglycan architecture (*e.g.* SGSH, CHST14, HSPG2); (2) antioxidant proteins (*e.g.* PARK7, PRDX1, TXN); and (3) LDHA, which was likely induced to deal with lactate accumulation in the medium because of tumor-related Warburg effect. Together this set of secreted proteins reveal that the effect of tumor cells on fibroblasts extends beyond mere activation of these cells, but also encompasses active influence over the production and extracellular deposition of proteins needed for lactate and ROS management. This agrees with the effects on tumor migration we observed (Fig. 2*E*, panel ❹), where conditioned medium harvested from activated fibroblasts induced pro-migratory phenotype in Hs578T cancer cells.

We further verified that activated fibroblasts promote tumor cell motility through counteracting oxidative stress associated with migration, by introducing ROS in the form of tert-butyl hydroperoxide (TBHP) or reduced glutathione (GSH) as antioxidant in migration assays (Fig. 7*C*). As shown in the right panel of Fig. 7*C*, tumor migration is enhanced in the presence of activated fibroblasts, or cell-free conditioned medium from activated fibroblasts (white and black bars). This indicated that the active ingredient from activated fibroblasts is secreted. When further challenged with TBHP, this migration advantage is lost (blue bar), which can be rescued with GSH antioxidant (red bar). We believe this shows that the change in migration behavior is not because of one specific functional protein species, but because of the collective antioxidant capacity of the secreted material. Based on quantitative comparison of nonactivated and activated fibroblast secretions (Fig. 7*A*), PARK7, LDHA, TXN, and PRDX1 emerge as the only differentially secreted proteins with known antioxidant function. Hence, we propose that

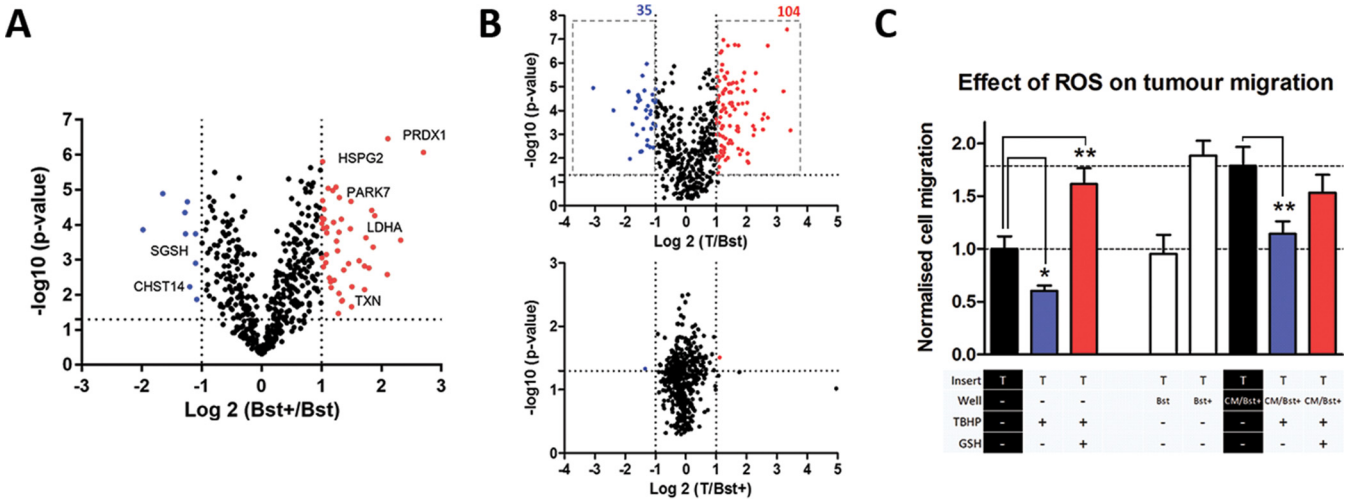

FIG. 7. **Activated fibroblasts promote tumor migration by counteracting oxidative stress.** *A*, Quantitative comparison of Hs578Bst and Hs578Bst+ secretomes ($n = 3$). Relative to nonactivated Hs578Bst fibroblasts, secretion of 48 proteins by activated Hs578Bst fibroblasts were increased by at least 2-fold (in red), whereas the secretion of 9 proteins (in blue) were reduced by at least 2-fold. Upon activation, Hs578Bst+ cells produced more antioxidants and LDHA, and altered the secretion of HSPG2 and sulfation enzymes. *B*, Secretome comparison of Hs578T cells with Hs578Bst and Hs578Bst+ cells ($n = 3$). Secretion profile of Hs578Bst+ was highly like that of Hs578T cells. *C*, Effect of antioxidants on Hs578T migration ($n = 3$). Hs578T migration was modulated positively or negatively by reduced glutathione (GSH) or tert-butylhydroperoxide (TBHP) respectively (Student's *t* test; $^{*}p < 0.05$; $^{**}p < 0.01$). Addition of TBHP eliminated the migratory advantage of Hs578T cells grown in Hs578Bst+ conditioned medium ($^{**}p < 0.01$; $n = 3$), whereas simultaneous addition of GSH was sufficient to rescue the phenotype.

micro-environmental modulations are likely mediated through these proteins.

More intriguingly, the secretome of fibroblasts after activation also becomes strikingly like that of the tumor cells. Secretion by tumor cells were rather different compared with nonactivated Hs578Bst fibroblasts (Fig. 7*B*, top), presumably because of the need to support a range of tumor processes from migration and invasion to the management of extracellular signaling and redox. However, upon activation, fibroblasts begin to mimic the secretion pattern of tumor cells to a high degree, such that almost no significant differences (>2-fold regulated; *t* test $p < 0.05$) were then noted between the Hs578T and Hs578Bst+ secretomes (Fig. 7*B*, bottom). This suggests that CTGF/VEGFA signaling from tumor cells also provides fibroblasts with instructions to phenocopy the tumor secretion profile, aimed at providing a favorable tissue microenvironment for tumor propagation.

DISCUSSION

To date, most studies investigating the role of fibroblasts in cancer begin with the assumption that activated fibroblasts promote tumor progression (20, 21), without addressing fully how fibroblasts become activated, or which specific processes the activated fibroblasts are involved in. Herein, we aimed to address these two critical questions. By searching for tumor-secreted fibroblast activators using fibroblast and tumor cells isolated from the same patient, we reconstituted *in vitro* a two-component fibroblast activating system involving CTGF and co-activator VEGFA and demonstrated that fibroblasts activated in this manner had functional consequences on tumor metastatic processes, mediated through micro-environmental modulation.

To avoid complex multi-way signaling between implanted fibroblasts, tumor cells and host fibroblasts that could significantly inflate experimental considerations, the activating functions of potential factors were tested in an *in vitro* system, containing only the tumor and fibroblasts. To minimize activation artifacts resulting from factor over-supplementation, we relied only on antibody-based factor retrieval from Hs578T tumor conditioned medium, where the yield was always within the physiological secreted concentration. To guard against false negatives, we circumvented the use of commercial purified proteins, which could fail to activate fibroblasts in the absence of critical post-translational modifications.

To our knowledge, CTGF and VEGFA have not been previously implicated in fibroblast activation. Although CTGF level is regulated via miRNA mechanisms in the contexts of liver pathology (22), diabetic nephropathy (23), and hyperplastic scar formation (24), these studies focused exclusively on autocrine effects, whereas the paracrine effect of tumor-secreted CTGF on other cell types in the tumor vicinity has not been studied. Similarly, VEGFA has a well-established role in tumor vascularization, but its function has not been linked to fibroblast activation, even though the duration of fibroblast activation appears to coincide well with the induction of new blood vessels prior to metastatic spread (17).

To explain the mechanism of tumor-dependent fibroblast activation, we consider the processes of CTGF docking and/or internalization by fibroblasts, downstream *Wnt* activa-

tion, and possible feedback loops that help to sustain the activated state. By plasma membrane fractionation and mass spectrometry, we detected expression and presentation of membrane *Wnt* co-receptors Lrp1, Lrp5, and Lrp6 on the fibroblast cell surface (Fig. 6*C*). We hypothesize that CTGF secreted by tumor cells may therefore dock on fibroblasts via interaction with Lrp1, which is known to function in CTGF transcytosis and redistribution within cartilage (25). We postulate that CTGF binding to Lrp5/6 may then occupy the *Wnt* co-receptors, to favor noncanonical *Wnt* signaling through Frizzled (Fzd) alone, via the ROCK and JNK routes (Fig. 6*C*). Such competitive Lrp5/6-independent Fzd-mediated mechanisms have been reported previously (26), and agree with the ROCK and JNK inhibition data presented here (Fig. 6*D*–6*E*). Upon activation, fibroblasts also increase the production of HSPG, which is known to interact with CTGF in the C terminus (27). This then can serve as additional mechanism to localize further CTGF to fibroblasts and sustain the activated state. Because we demonstrate experimentally that CTGF and VEGFA interact extracellularly (Fig. 6A), it is possible that CTGF binding and internalization processes also accounts for the uptake and activity of VEGFA in part.

N-terminal CTGF has also been reported to mediate TGFβ and BMP signaling (27). Nonetheless, the paracrine fibroblast activation we report here appears to be independent of TGFβ (Fig. 6*C*). We arrive at this conclusion considering that (1) addition of TGFβ and LTBP1, or Gsk3 inhibitor had no impact on fibroblast activation (Fig. 4*B*, supplemental Fig. S6); (2) levels of phosphorylated Akt1, Smad2, Smad3, and Src were not significantly changed upon fibroblast activation (supplemental Fig. S2*B*); (3) collagen production downstream of IGF pathways was not increased but suppressed in activated fibroblasts (supplemental Fig. S2*A*). Collectively, these provide evidence that contrary to the postulated role of TGFβ in fibroblast activation (28), the paracrine activation we observe here is largely mediated through the C-terminal half of CTGF. Coherent with this, frequent N-terminal proteolytic processing of CTGF *in vivo* by MMPs (29) also limits the role of N-terminal CTGF as a paracrine fibroblast activator.

Apart from CTGF/VEGFA that we report here, several other potential fibroblast activators have been suggested to date but with little to no overlap between studies. Compared with putative fibroblast activators in literature, we did not detect Wnt7a (30), Twist-1 (31) or HSF1 (32) secretion from the HS578T cells. We believe this result largely from the highly heterologous systems used in these earlier studies. Pairing fibroblasts from mouse with human tumor cells for example cannot fully recapitulate the intercellular signaling within a human patient (33). Similarly, organ specificity is another critical consideration when pairing fibroblasts with tumors obtained from the same host. This is because fibroblasts from a specific organ could express a unique repertoire of receptors that respond only to organ-specific ligands; tumor cells on the other hand may also require the support of specific growth factors derived only from the native tissue context. As such, organ specificity is a critical consideration in investigations dealing with tumor-fibroblast crosstalk, and the only physiological way to study fibroblast activation is to use fibroblasts isolated from the same patient in spatial proximity to the tumor cells as we did here.

In the literature, the term "fibroblast activation" has been used widely to describe morphological and behavioral changes in fibroblasts induced by diverse stimuli. Based on the secretion profile and growth characteristics, we further distinguish the fibroblast activation reported here from those implicated in wound healing processes and senescence (34). Hyperactive ECM deposition is an invariant cancer phenotype. Hence tumors have been described as "overhealing wounds" (35) and "wounds that never heal" (36) respectively, because of the massive and persistent production of collagens at tumor sites. In contrast, we did not observe experimentally excessive ECM production by the activated fibroblasts. In fact, the secretions of many collagens were decreased upon Hs578Bst activation by CTGF/VEGFA (supplemental Fig. S4*B*), suggesting that tumor-dependent fibroblast activation could give rise to yet another distinct fibroblast entity apart from those described in healing wounds and senescent contexts. Indeed, the secretion profile we observed in activated Hs578Bst+ cells was also not characteristic of the senescence associated secretory phenotype (SASP) described previously (37), although SASP has also been suggested to promote tumor progression (38).

Several recent reports have described autonomous "division-of-labor" between sub-populations of cancer cells within the same tumor (39–42). These studies focused largely on demonstrating intra-tumor specialization and cooperation, where malignant sub-populations with genetic alterations conferring growth advantage or survival fitness work together as a tumor system. We show here, on the other hand, an intriguing commensal relationship where tumor cells exert active influence over a noncancer cell type in the microenvironment, to create conditions favorable for metastasis ahead of their eminent spread. In this context, Hs578T tumor cells appear to delegate the critical task of micro-environmental modulation to fibroblasts in the vicinity through the CTGF/VEGFA-dependent activation process, to manage tumor acidification because of Warburg effect and simultaneously mitigate the inhibition of local oxidative stress on tumor cell migration. The findings presented here thus broaden the perspective that division-of-labor could also exist between normal and cancer cells, under the directive of the latter. Activated fibroblasts are also present in large numbers at tumor sites, therefore even small changes in secretion could become amplified by a community effect.

More intriguingly, activation of fibroblasts by CTGF/VEGFA also altered the apparent production of HSPG2 and enzymes modulating sulfation on the cell surface (Fig. 7A). SGSH cat-

alyzes the degradation of heparan sulfate (43), a prominent modification found on the plasma membrane of breast cancer cells. Cell surface heparan sulfate proteoglycans (HSPGs) have been shown to control adhesion and invasion in breast cancer (44) and impact growth factor signaling under the tight regulation of sulfyltransferases, sulfatases and heparanases (45). CHST14 sulfo-transferase on the other hand regulates membrane chondroitin and dermatan sulfate content (46). Chondroitin sulfate proteoglycans (CSPGs) have been implicated in tumor metastasis (47) and are also associated with poor clinical outcome in breast cancer (48). The identification of secreted SGSH and CHST14 appears to suggest that post-Golgi processing or modulation of sulfated proteoglycans after membrane presentation may be possible, although no mechanisms for this have been reported thus far. It is also unclear at this point if the substrate for these secreted enzymes reside on the surface of tumor cells or on fibroblasts, but this potentially adds yet another dimension to the functional consequences of tumor-dependent fibroblast activation, pending further investigations.

It is even more crucial to highlight that the fibroblast activation we report here is reversible, unlike intra-tumor heterogeneity driven by mutations. This implies that therapeutic intervention against the activation process or preventing the sustenance of fibroblast activated state could potentially reduce metastatic spread as an adjuvant following surgical resection. We show here for this purpose, that a CTGF antibody effectively blocks fibroblast activation *in vitro*. Related to this finding, a cyclic RGD penta-peptide has been reported to block CTGF in the context of glaucoma therapy (49), and a humanized CTGF single-chain variable fragment (ScFv) antibody FG-3019 has been tested with positive outcome, in Phase II clinical trials for the treatment of fibrosis (50). These are potentially good starting points for clinical CTGF inhibition, in the alternative context of breast cancer-associated fibroblast activation.

In conclusion, we report here that tumor-secreted CTGF/VEGFA have profound activating effects on fibroblast metabolism and secretion, and reciprocal signaling from activated fibroblasts prepares the microenvironment for tumor dissemination through the provision of antioxidants and lactate detoxifying capacities (Fig. 8). This work contributes further refinement to the "seed and soil hypothesis" proposed more than two decades ago (51), aptly also in the context of breast cancer, where cancer cells now dispatch instructions to make their own fertile ground. Signaling plasticity in the tumor microenvironment is an increasingly recognized and important factor to consider in cancer therapy. Our data here suggests that disrupting the tumor-fibroblast interactions could be a viable strategy to eliminate the survival and metastatic support a tumor receives from the tissue microenvironment.

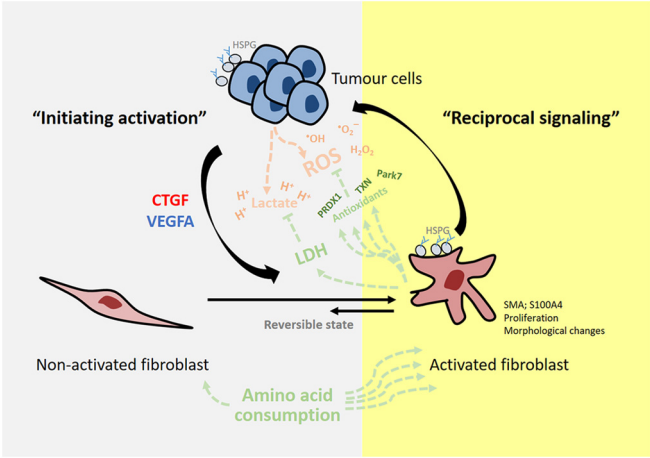

FIG. 8. **Summary: Tumor-dependent fibroblast activation at a glance.** Fibroblast activation is reversible and requires tumor-derived CTGF and VEGFA. Activated fibroblasts in turn promote migration of cancer cells by increasing amino acid uptake, to synthesize and secrete proteins that mitigate micro-environmental stress from lactate and ROS accumulation. Gray: initiation of fibroblast activation; yellow: reciprocal signaling from activated fibroblast back to tumor cells. Extracellular agents in orange: lactate and pro-oxidants (peroxide, ROS and radical oxygen species); and in green: LDH and antioxidants (PRDX1, TXN and Park7).

DATA AVAILABILITY

MS raw files were deposited to the public database ProteomeXchange via the PRIDE partner repository (http://proteomecentral.proteomexchange.org), as project PXD007898.

* This work was supported by *Proteins@Work*, a program of the Netherlands Proteomics Centre financed by the Netherlands Organisation for Scientific Research (NWO) as part of the National Roadmap Large-scale Research Facilities of the Netherlands (project number 184.032.201). SL acknowledges support from the Netherlands Organisation for Scientific Research (NWO) through a VIDI grant (project number 723.013.008). CRB acknowledges support from the Netherlands Organization for Scientific Research (NWO) through a VENI grant (project number 722.013.009).

[S] This article contains supplemental material.

¶ To whom correspondence should be addressed: Biomolecular Mass Spectrometry and Proteomics, Bijvoet Center for Biomolecular Research and Utrecht Institute for Pharmaceutical Sciences, Utrecht University, Padualaan 8, 3584 CH Utrecht, the Netherlands. E-mail: a.j.r.heck@uu.nl.

Author contributions: W.W. designed research; W.W. and E.A.Z. performed research; W.W. analyzed data; W.W., S.L., and A.J.R.H. wrote the paper; C.R.B. contributed new reagents/analytic tools; C.R.B. metabolomics; S.L. and A.J.R.H. supervision.

REFERENCES

1. Bhowmick, N. A., Neilson, E. G., and Moses, H. L. (2004) Stromal fibroblasts in cancer initiation and progression. *Nature* **432,** 332–337
2. Obenauf, A. C., Zou, Y., Ji, A. L., Vanharanta, S., Shu, W., Shi, H., Kong, X., Bosenberg, M. C., Wiesner, T., Rosen, N., Lo, R. S., and Massague, J. (2015) Therapy-induced tumour secretomes promote resistance and tumour progression. *Nature* **520,** 368–372
3. Webber, J. P., Spary, L. K., Sanders, A. J., Chowdhury, R., Jiang, W. G., Steadman, R., Wymant, J., Jones, A. T., Kynaston, H., Mason, M. D., Tabi, Z., and Clayton, A. (2015) Differentiation of tumour-promoting stromal myofibroblasts by cancer exosomes. *Oncogene* **34,** 290–302

4. Nguyen-Ngoc, K. V., Cheung, K. J., Brenot, A., Shamir, E. R., Gray, R. S., Hines, W. C., Yaswen, P., Werb, Z., and Ewald, A. J. (2012) ECM microenvironment regulates collective migration and local dissemination in normal and malignant mammary epithelium. *Proc. Natl. Acad. Sci. U.S.A.* **109,** E2595–E2604
5. Kammertoens, T., Schuler, T., and Blankenstein, T. (2005) Immunotherapy: target the stroma to hit the tumour. *Trends Mol. Med.* **11,** 225–231
6. Motaln, H., Gruden, K., Hren, M., Schichor, C., Primon, M., Rotter, A., and Lah, T. T. (2012) Human mesenchymal stem cells exploit the immune response mediating chemokines to impact the phenotype of glioblastoma. *Cell Transplant* **21,** 1529–1545
7. Sharma, P., and Allison, J. P. (2015) Immune checkpoint targeting in cancer therapy: toward combination strategies with curative potential. *Cell* **161,** 205–214
8. Zins, K., Sioud, M., Aharinejad, S., Lucas, T., and Abraham, D. (2015) Modulating the tumour microenvironment with RNA interference as a cancer treatment strategy. *Methods Mol. Biol.* **1218,** 143–161
9. Buchheit, C. L., Weigel, K. J., and Schafer, Z. T. (2014) Cancer cell survival during detachment from the ECM: multiple barriers to tumour progression. *Nat. Rev. Cancer* **14,** 632–641
10. Wolf, K., and Friedl, P. (2011) Extracellular matrix determinants of proteolytic and non-proteolytic cell migration. *Trends Cell Biol.* **21,** 736–744
11. Piskounova, E., Agathocleous, M., Murphy, M. M., Hu, Z., Huddlestun, S. E., Zhao, Z., Leitch, A. M., Johnson, T. M., DeBerardinis, R. J., and Morrison, S. J. (2015) Oxidative stress inhibits distant metastasis by human melanoma cells. *Nature* **527,** 186–191
12. Cao, H., Eppinga, R. D., Razidlo, G. L., Krueger, E. W., Chen, J., Qiang, L., and McNiven, M. A. (2016) Stromal fibroblasts facilitate cancer cell invasion by a novel invadopodia-independent matrix degradation process. *Oncogene* **35,** 1099–1110
13. Eichelbaum, K., Winter, M., Berriel Diaz, M., Herzig, S., and Krijgsveld, J. (2012) Selective enrichment of newly synthesized proteins for quantitative secretome analysis. *Nat. Biotechnol.* **30,** 984–990
14. Giansanti, P., Tsiatsiani, L., Low, T. Y., and Heck, A. J. (2016) Six alternative proteases for mass spectrometry-based proteomics beyond trypsin. *Nat. Protoc.* **11,** 993–1006
15. de Graaf, E. L., Giansanti, P., Altelaar, A. F., and Heck, A. J. (2014) Single-step enrichment by Ti4+-IMAC and label-free quantitation enables in-depth monitoring of phosphorylation dynamics with high reproducibility and temporal resolution. *Mol. Cell. Proteomics* **13,** 2426–2434
16. Yu, Y., Xiao, C. H., Tan, L. D., Wang, Q. S., Li, X. Q., and Feng, Y. M. (2014) Cancer-associated fibroblasts induce epithelial-mesenchymal transition of breast cancer cells through paracrine TGF-beta signalling. *Br. J. Cancer* **110,** 724–732
17. Kalluri, R. (2016) The biology and function of fibroblasts in cancer. *Nat Rev. Cancer* **16,** 582–598
18. Uhlen, M., Oksvold, P., Fagerberg, L., Lundberg, E., Jonasson, K., Forsberg, M., Zwahlen, M., Kampf, C., Wester, K., Hober, S., Wernerus, H., Bjorling, L., and Ponten, F. (2010) Towards a knowledge-based Human Protein Atlas. *Nat. Biotechnol.* **28,** 1248–1250
19. Yu, O. M., and Brown, J. H. (2015) G protein-coupled receptor and RhoA-stimulated transcriptional responses: links to inflammation, differentiation, and cell proliferation. *Mol. Pharmacol.* **88,** 171–180
20. Calvo, F., Ranftl, R., Hooper, S., Farrugia, A. J., Moeendarbary, E., Bruckbauer, A., Batista, F., Charras, G., and Sahai, E. (2015) Cdc42EP3/BORG2 and Septin Network Enables Mechano-transduction and the Emergence of Cancer-Associated Fibroblasts. *Cell Rep.* **13,** 2699–2714
21. Erez, N., Truitt, M., Olson, P., Arron, S. T., and Hanahan, D. (2010) Cancer-Associated Fibroblasts Are Activated in Incipient Neoplasia to Orchestrate Tumour-Promoting Inflammation in an NF-kappaB-Dependent Manner. *Cancer Cell* **17,** 135–147
22. Gjymishka, A., Pi, L., Oh, S. H., Jorgensen, M., Liu, C., Protopapadakis, Y., Patel, A., and Petersen, B. E. (2016) miR-133b Regulation of Connective Tissue Growth Factor: A Novel Mechanism in Liver Pathology. *Am. J. Pathol.* **186,** 1092–1102
23. Wang, J., Duan, L., Guo, T., Gao, Y., Tian, L., Liu, J., Wang, S., and Yang, J. (2016) Downregulation of miR-30c promotes renal fibrosis by target CTGF in diabetic nephropathy. *J. Diabetes Complications* **30,** 406–414
24. Mu, S., Kang, B., Zeng, W., Sun, Y., and Yang, F. (2016) MicroRNA-143–3p inhibits hyperplastic scar formation by targeting connective tissue growth factor CTGF/CCN2 via the Akt/mTOR pathway. *Mol. Cell. Biochem.* **416,** 99–108
25. Kawata, K., Kubota, S., Eguchi, T., Aoyama, E., Moritani, N. H., Kondo, S., Nishida, T., and Takigawa, M. (2012) Role of LRP1 in transport of CCN2 protein in chondrocytes. *J. Cell Sci.* **125,** 2965–2972
26. Li, X., Zhang, Y., Kang, H., Liu, W., Liu, P., Zhang, J., Harris, S. E., and Wu, D. (2005) Sclerostin binds to LRP5/6 and antagonizes canonical Wnt signaling. *J. Biol. Chem.* **280,** 19883–19887
27. Lipson, K. E., Wong, C., Teng, Y., and Spong, S. (2012) CTGF is a central mediator of tissue remodeling and fibrosis and its inhibition can reverse the process of fibrosis. *Fibrogenesis Tissue Repair* **5,** S24
28. Chen, H., Yang, W. W., Wen, Q. T., Xu, L., and Chen, M. (2009) TGF-beta induces fibroblast activation protein expression; fibroblast activation protein expression increases the proliferation, adhesion, and migration of HO-8910PM [corrected]. *Exp. Mol. Pathol.* **87,** 189–194
29. Gao, R., and Brigstock, D. R. (2003) Low density lipoprotein receptor-related protein (LRP) is a heparin-dependent adhesion receptor for connective tissue growth factor (CTGF) in rat activated hepatic stellate cells. *Hepatol. Res.* **27,** 214–220
30. Avgustinova, A., Iravani, M., Robertson, D., Fearns, A., Gao, Q., Klingbeil, P., Hanby, A. M., Speirs, V., Sahai, E., Calvo, F., and Isacke, C. M. (2016) Tumour cell-derived Wnt7a recruits and activates fibroblasts to promote tumour aggressiveness. *Nat. Commun.* **7,** 10305
31. Garcia-Palmero, I., Torres, S., Bartolome, R. A., Pelaez-Garcia, A., Larriba, M. J., Lopez-Lucendo, M., Pena, C., Escudero-Paniagua, B., Munoz, A., and Casal, J. I. (2016) Twist1-induced activation of human fibroblasts promotes matrix stiffness by upregulating palladin and collagen alpha1(VI). *Oncogene* **35,** 5224–5236
32. Scherz-Shouval, R., Santagata, S., Mendillo, M. L., Sholl, L. M., Ben-Aharon, I., Beck, A. H., Dias-Santagata, D., Koeva, M., Stemmer, S. M., Whitesell, L., and Lindquist, S. (2014) The reprogramming of tumour stroma by HSF1 is a potent enabler of malignancy. *Cell* **158,** 564–578
33. Stuelten, C. H., DaCosta Byfield, S., Arany, P. R., Karpova, T. S., Stetler-Stevenson, W. G., and Roberts, A. B. (2005) Breast cancer cells induce stromal fibroblasts to express MMP-9 via secretion of TNF-alpha and TGF-beta. *J. Cell Sci.* **118,** 2143–2153
34. Wagner, E. F. (2016) Cancer: Fibroblasts for all seasons. *Nature* **530,** 42–43
35. Schafer, M., and Werner, S. (2008) Cancer as an overhealing wound: an old hypothesis revisited. *Nat. Rev. Mol. Cell Biol.* **9,** 628–638
36. Dvorak, H. F. (1986) Tumours: wounds that do not heal. Similarities between tumour stroma generation and wound healing. *N. Engl. J. Med.* **315,** 1650–1659
37. Coppe, J. P., Desprez, P. Y., Krtolica, A., and Campisi, J. (2010) The senescence-associated secretory phenotype: the dark side of tumour suppression. *Annu. Rev. Pathol.* **5,** 99–118
38. Campisi, J. (2005) Senescent cells, tumour suppression, and organismal aging: good citizens, bad neighbors. *Cell* **120,** 513–522
39. Tape, C. J., Ling, S., Dimitriadi, M., McMahon, K. M., Worboys, J. D., Leong, H. S., Norrie, I. C., Miller, C. J., Poulogiannis, G., Lauffenburger, D. A., and Jorgensen, C. (2016) Oncogenic KRAS regulates tumour cell signaling via stromal reciprocation. *Cell* **165,** 910–920
40. Meacham, C. E., and Morrison, S. J. (2013) Tumour heterogeneity and cancer cell plasticity. *Nature* **501,** 328–337
41. Greaves, M., and Maley, C. C. (2012) Clonal evolution in cancer. *Nature* **481,** 306–313
42. Beca, F., and Polyak, K. (2016) Intratumour heterogeneity in breast cancer. *Adv. Exp. Med. Biol.* **882,** 169–189
43. Scott, H. S., Blanch, L., Guo, X. H., Freeman, C., Orsborn, A., Baker, E., Sutherland, G. R., Morris, C. P., and Hopwood, J. J. (1995) Cloning of the sulphamidase gene and identification of mutations in Sanfilippo A syndrome. *Nat. Genet.* **11,** 465–467
44. Lim, H. C., Multhaupt, H. A., and Couchman, J. R. (2015) Cell surface heparan sulfate proteoglycans control adhesion and invasion of breast carcinoma cells. *Mol. Cancer* **14,** 15
45. Knelson, E. H., Nee, J. C., and Blobe, G. C. (2014) Heparan sulfate signaling in cancer. *Trends Biochem. Sci.* **39,** 277–288
46. Pacheco, B., Maccarana, M., and Malmstrom, A. (2009) Dermatan 4-O-sulfotransferase 1 is pivotal in the formation of iduronic acid blocks in dermatan sulfate. *Glycobiology* **19,** 1197–1203

47. Cooney, C. A., Jousheghany, F., Yao-Borengasser, A., Phanavanh, B., Gomes, T., Kieber-Emmons, A. M., Siegel, E. R., Suva, L. J., Ferrone, S., Kieber-Emmons, T., and Monzavi-Karbassi, B. (2011) Chondroitin sulfates play a major role in breast cancer metastasis: a role for CSPG4 and CHST11 gene expression in forming surface P-selectin ligands in aggressive breast cancer cells. *Breast Cancer Res.* **13,** R58
48. Svensson, K. J., Christianson, H. C., Kucharzewska, P., Fagerstrom, V., Lundstedt, L., Borgquist, S., Jirstrom, K., and Belting, M. (2011) Chondroitin sulfate expression predicts poor outcome in breast cancer. *Int. J. Oncol.* **39,** 1421–1428
49. Hennig, R., Kuespert, S., Haunberger, A., Goepferich, A., and Fuchshofer, R. (2016) Cyclic RGD peptides target human trabecular meshwork cells while ameliorating connective tissue growth factor-induced fibrosis. *J. Drug Target* **24,** 950–959
50. Raghu, G., Scholand, M. B., de Andrade, J., Lancaster, L., Mageto, Y., Goldin, J., Brown, K. K., Flaherty, K. R., Wencel, M., Wanger, J., Neff, T., Valone, F., Stauffer, J., and Porter, S. (2016) FG-3019 anti-connective tissue growth factor monoclonal antibody: results of an open-label clinical trial in idiopathic pulmonary fibrosis. *Eur. Respir. J.* **47,** 1481–1491
51. Paget, S. (1989) The distribution of secondary growths in cancer of the breast. 1889. *Cancer Metastasis Rev.* **8,** 98–101